

Telomere Maintenance-Associated PML Is a Potential Specific Therapeutic Target of Human Colorectal Cancer



Peng Gong^{a,b,1}, Hua Wang^{a,b,1}, Jingsong Zhang^c, Yudong Fu^{a,b,1}, Zhengmao Zhu^{a,b}, Jinmiao Wang^c, Yu Yin^{a,b}, Haiying Wang^{a,b}, Zhongcheng Zhou^{a,b}, Jiao Yang^{a,b}, Linlin Liu^{a,b}, Mo Gou^{a,b}, Ming Zeng^{a,b}, Jinghua Yuan^d, Feng Wang^d, Xinghua Pan^e, Rong Xiang^a, Sherman M. Weissman^e, Feng Qi^c and Lin Liu^{a,b}

^aState Key Laboratory of Medicinal Chemical Biology, 2011 Collaborative Innovation Center for Biotherapy;

^bDepartment of Cell Biology and Genetics, College of Life Sciences, Nankai University, Tianjin, 300071, China;

^cDepartment of General Surgery, Tianjin Medical University General Hospital, Tianjin, 300052, China; ^dDepartment of Genetics, Tianjin Medical University, Tianjin, 300070, China;

^eDepartment of Genetics, Yale School of Medicine, New Haven, CT, 06520, USA

Abstract

Telomere length maintenance is essential for cell proliferation, which is particularly prominent in cancer. We validate that the primary colorectal tumors exhibit heterogeneous telomere lengths but mostly (90%) short telomeres relative to normal tissues. Intriguingly, relatively short telomeres are associated with tumor malignancy as indicated by poorly differentiated state, and these tumors contain more cancer stem-like cells (CSLCs) identified by several commonly used markers CD44, EPHB2 or LGR5. Moreover, promyelocytic leukemia (PML) and ALT-associated PML nuclear bodies (APBs) are frequently found in tumors with short telomeres and high proliferation. In contrast, distant normal tissues rarely or only minimally express PML. Inhibition of PML and APBs by an ATR inhibitor decreases proliferation of CSLCs and organoids, suggesting a potential therapeutic target to progressive colorectal tumors. Together, telomere maintenance underlying tumor progression is connected with CSLCs.

Translational Oncology (2019) 12, 1164–1176

Introduction

Colorectal cancer (CRC) is the third most common cause of new cancer cases and death [1]. One of the greatest challenges to cancer treatment is the tumor heterogeneity and the existence of cancer stem cells (CSCs) or cancer stem-like cells (CSLCs) in various subpopulations [2–5]. CSCs possess self-renewal potential and can initiate a full malignant cell population. CSCs may differ in susceptibility to therapy from the bulk of the tumor cells, limiting the effectiveness of cancer therapies [4,6–8]. Expression of CSCs markers, CD44, EPHB2 (Eph receptor B2) and LGR5 (leucine rich repeat containing G protein-coupled receptor 5) which are also WNT target genes [8–13], indicates activation of WNT signaling pathway and advanced disease [14–16].

Telomere shortening promotes chromosomal/genomic instability and drives malignant transformation during the early stage of

carcinogenesis, including CRCs [17–22]. At some points, the telomere length has to be maintained or stabilized for cell self-renewal and replication [23], and otherwise telomere attrition would

Address all correspondence to: Feng Qi, Department of General Surgery, Tianjin Medical University General Hospital, Tianjin, China. or Lin Liu, Department of Cell Biology and Genetics, College of Life Sciences, Nankai University, Tianjin, China. E-mail: qf@medmail.com.cn

¹These authors contributed equally to this work. Received 9 May 2019; Accepted 13 May 2019

© 2019 The Authors. Published by Elsevier Inc. on behalf of Neoplasia Press, Inc. This is an open access article under the CC BY-NC-ND license (<http://creativecommons.org/licenses/by-nc-nd/4.0/>).

1936-5233/19

<https://doi.org/10.1016/j.tranon.2019.05.010>

cause cell senescence or death. Telomere length primarily is maintained by telomerase, which is composed of two core components *TERT* and *TERC* [24]. Telomerase is highly expressed in embryonic tissues, but is silent in the vast majority of human tissues following differentiation [25]. Telomerase and particularly *TERT* are reactivated in about 90% of human tumors, and maintain telomere lengths and tumor growth [26,27]. Telomeres also can be elongated by alternative lengthening of telomeres pathways (ALT) based on homologous recombination, involving promyelocytic leukemia (PML) body at telomeres [28–31]. Previous researches on telomeres in CRCs mostly focus on the correlations between telomere length, telomerase, and prognosis [22,32–38]. Moreover, existence of ALT and the associated PML in primary CRCs are also revealed [39,40], but without systematic analysis and functional test of the connection to underlying tumor progression state and involvement of CSCs. It remains elusive how telomeres lengths are varied and maintained during tumor progression of CRCs.

Given that the primary human tumors are the most appropriate sources for studying CSC subpopulations *in situ* that exist prior to their isolation from patients [4], we performed comprehensive analysis of telomere lengths and searched in the CRC primary tumors for CSLCs characterized by commonly used cell surface markers. Our data suggest that PML bodies together with telomerase are implicated in the maintenance of telomeres of highly proliferative CRC tumors. Patient-derived organoids (PDOs) have recently emerged as robust models to mimic *in vivo* experiments and predict clinical outcomes in patients [41–44]. Our data further support the notion that specific target to telomere maintenance provides a promising direction for CSCs inhibition and CRC tumor therapy.

Materials and Methods

Patients and Tissue Samples

Primary colorectal carcinomas and their corresponding control tissue samples adjacent or distant to tumor were obtained from patients who underwent surgery at Tianjin Medical University General Hospital. This study was approved by the Ethical Committee at Tianjin Medical University General Hospital (Ethical No. IRB2014-YX-041), and informed consent obtained prior to investigation (Supplemental Experimental Procedures). Paired adjacent and distant non-cancerous, presumably 'normal' tissues from the same patient served as controls were obtained 5 cm and 10 cm respectively away from the distal margin of the tumor. The histological classification of tumors was established according to previous criteria, based on the dominant pattern (Clinical information is provided in Supplementary Table 1). None of the patients had received neoadjuvant therapy prior to surgical resection. Samples were frozen within 1h and were kept in liquid nitrogen until used for extraction of DNA, RNA, protein or frozen sectioning. Fresh samples were delivered on ice, fixed in 3.7% paraformaldehyde and embedded in paraffin sections. Normal colon sample and ulcerative colitis patient sample were collected as controls.

Telomere Measurement by Quantitative Real-Time PCR

Average telomere length was measured using real-time PCR assay, as previously described [45] (Supplementary Experimental Procedures). Genomic DNA from different cancer samples was isolated with DNeasy Blood & Tissue kit (69504, Qiagen), and 1.5 µg DNA digested using Hinf I and Rsa I restriction enzymes. Digested DNA

underwent electrophoresis through a 0.8% agarose gel (111860, Biowest) for 4h at 6 V/cm in the 1 × TAE buffer. Gels were denatured, neutralized, and transferred to positively charged nylon membranes (RPN2020B, GE Healthcare) overnight. The membranes were hybridized in DIG Easy Hyb containing the telomere probe at 42°C overnight. The mean terminal restriction fragment (TRF) length was quantitatively measured according to the kit instructions.

TRF by Southern Blot Analysis

Telomere terminal restriction fragment (TRF) analysis was performed using a commercial kit (TeloTAGGG Telomere Length Assay, 12209136001, Roche Life Science) (Supplemental Experimental Procedures).

Telomere Quantitative Fluorescence In Situ Hybridization (QFISH)

Tissues were frozen in liquid nitrogen, embedded in optimum cutting temperature compound (SAKURA Tissue-Tek O.C.T.), and cut into 7 µm sections. Telomere FISH and quantification were performed as described previously [46], except for FITC-labeled (CCCTAA)₃ peptide nucleic acid (PNA) probe (Panagene, Korea) used in this study. Telomeres were denatured at 80 °C for 3 min and hybridized with telomere PNA probe (0.5 µg/ml). Fluorescence from chromosomes and telomeres was digitally imaged on Zeiss Axio Imager Z2 microscope with FITC/DAPI filters, using AxioCam and AxioVision software 4.6. Exposure time for fluorescence signals of telomeres and other markers was kept consistent among different sections and tissues. For quantitative measurement of telomere length, telomere fluorescence intensity was integrated using the TFL-TELO program (gift kindly provided by P. Lansdorp).

Organoid Culture and Treatment

Organoids were established according to published protocols [41,43,47] (Supplementary Experimental Procedures).

Statistical Analysis

SPSS version 17.0 was used for statistical analysis. Correlation between telomere length and age was examined using Pearson's correlation coefficient. Colorectal tumors were divided into two or three groups according to their telomere length obtained by qPCR. Clinical data and T/S ratios were compared among these groups. Statistics was performed by analysis of variance and means and compared by Fisher's protected least-significant difference. A value of $P < .05$ was considered statistical significance.

Results

CRC Tumors Exhibit Heterogeneous Short Telomeres and are Independent of Age

Initially, we measured telomere lengths of the tumors, adjacent tissues and distant tissues from 54 patients and also of peripheral blood from 20 patients by a qPCR-based method (Table S1). Most tumors exhibited shorter telomeres than did those of adjacent and distant 'normal' tissues (T/S ratio ranging from 0.74 to 0.98, 47 out of 54, 87%), and only a few tumors showed relatively long telomeres similar to distant tissues (1.01 to 1.19, 7 out of 54, 13%). Adjacent and distant tissues maintained homogeneous telomere lengths (Figure 1A). Tumors showed telomere length heterogeneity with a wide range

of distribution (0.899 ± 0.083), unlike adjacent and distant 'normal' tissues (Table S1). By paired-samples T test, telomeres of tumors were significantly shorter than those of adjacent and distant tissues ($P <$

.001) and blood ($P = .0012$) (Figure 1B). An ulcerative colitis patient also displayed shorter telomeres in inflamed tissue, consistent with a previous study [48].

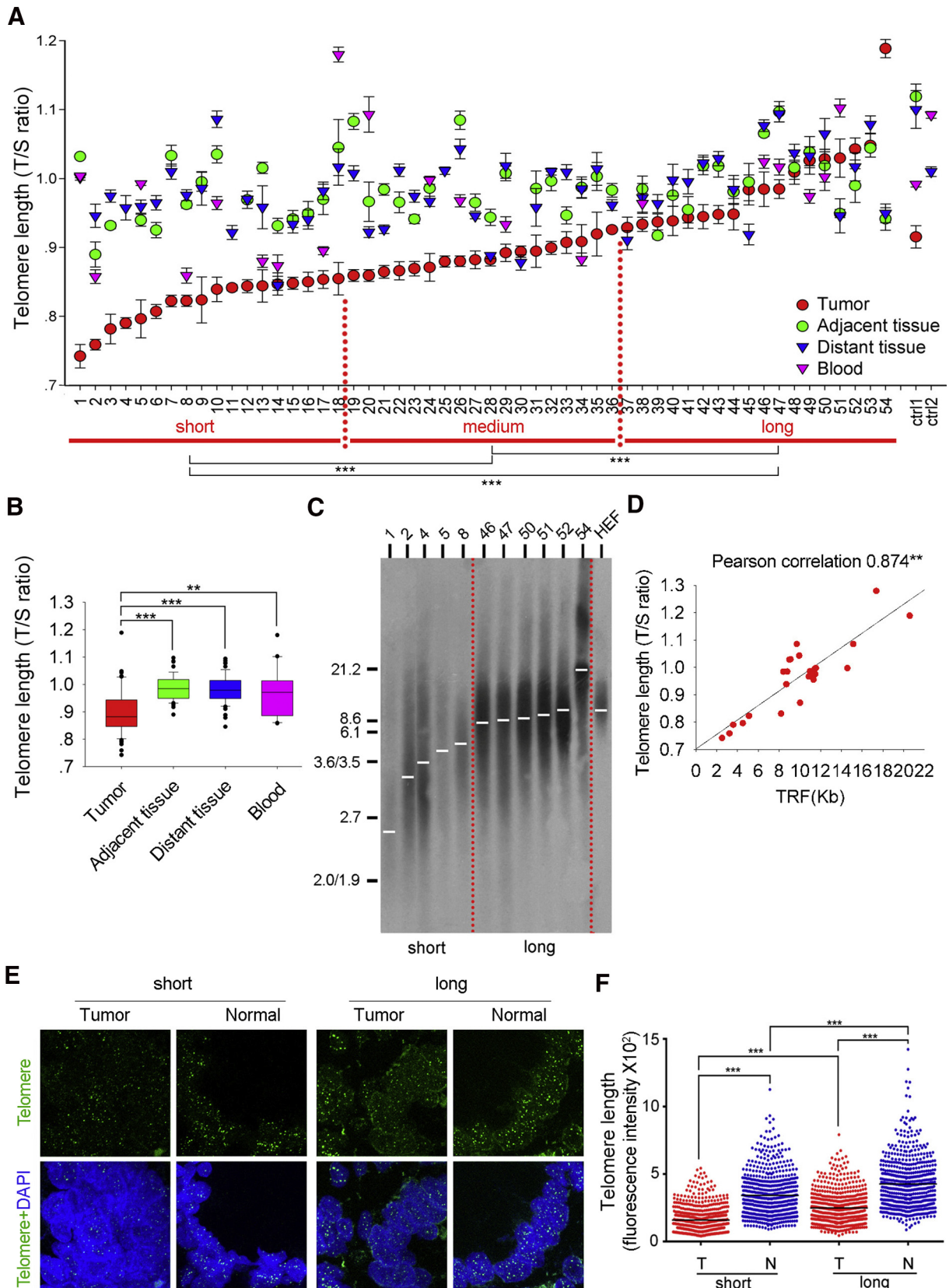


Table 1. Association between clinical variables and telomere lengths in colorectal cancer.

Parameter	NO.	Telomere length of tumor			P
		Short	Medium	Long	
Age (years)	50	16	17	17	.826
<64	26	8	8	10	
≥64	24	8	9	7	
Gender	50	16	17	17	.629
Female	29	11	9	9	
Male	21	5	8	8	
Tumor site	50	16	17	17	.044
Right colon	23	5	7	11	
Left colon	15	6	8	1	
Others	12	5	2	5	
Histology	44	15	13	16	.049
Poor	6	2	3	1	
Moderate	20	10	2	8	
Well	18	3	8	7	
Tumor size *	40	14	12	14	.247
≤4 cm	11	2	3	6	
>4 cm	29	12	9	8	
Depth of invasion (T)	46	15	14	17	.715
Tis + T2	2	0	1	1	
T4a	41	13	13	15	
T4b	3	2	0	1	
Lymph node involvement (N)	46	15	14	17	.340
N0	29	7	11	11	
N1a	7	3	1	3	
N1b	4	2	1	1	
N2a	4	3	1	0	
N2b	2	0	0	2	
Metastasis (M)	46	15	14	17	.496
M0	41	12	13	16	
M1	5	3	1	1	
TNM staging	45	15	13	17	.510
Stage II	28	7	10	11	
Stage III	12	5	2	5	
Stage IV	5	3	1	1	
Dukes classification	40	12	12	16	.473
B	28	7	10	11	
C	12	5	2	5	
CEA (ng/ml)	35	9	13	13	.318
<5	20	3	8	9	
≥5	15	6	5	4	

Patients were split into three groups based on telomere length in tumor: short (sTL), medium (mTL) and long telomere length (ITL) group, with each consisting of 18 patients. Four patients' clinical information not available, so not include in this analysis.

* J. O'Sullivan, R.A. Risques, M.T. Mandelson, L. Chen, T.A. Brentnall, M.P. Bronner, M.P. Macmillan, Z. Feng, J.R. Siebert, J.D. Potter, P.S. Rabinovitch, Telomere length in the colon declines with age: a relation to colorectal cancer?, Cancer Epidemiol Biomarkers Prev, 15 (2006) 573-577.

We then measured telomere lengths by telomere terminal restriction fragment measurement (TRF) (Figure 1C), the gold standard of telomere length measurement. Telomere length, shown as T/S ratio, was highly correlated with TRF result (Figure 1D). Telomere length shown as T/S ratio was also validated by telomere quantitative fluorescence *in situ* hybridization (QFISH). Telomeres of tumors were significantly shorter than those of distant 'normal' tissues (Figure 1, E and F). Telomeres of tumors in the long telomere

group were longer than those of the short telomere group ($P < .001$) (Figure 1F). Regardless of the potential variations, the average telomeres were shorter in tumors than in distant normal tissues estimated by QFISH, consistent with T/S ratio data.

Then we analyzed whether patients' age influences telomere lengths of tumors. Correlation between telomere length and age was examined using Pearson's correlation coefficient. Significant inverse correlations were found between age and telomere length in adjacent ($P = .001$) (Figure S1A) and distant 'normal' tissues ($P = .046$) (Figure S1B), indicating age-associated telomere shortening in non-tumor tissues, and supporting the general view of telomere shortening with age. Interestingly, telomere length of tumors did not shorten with age of the patient ($P = .365$) (Figure S1C), suggesting a distinct mechanism for telomere maintenance in tumorigenesis.

Relatively Short Telomeres are Associated with Malignancy

To further investigate potential links between telomere length and clinicopathological characteristics, 54 patients were split into three groups based on telomere length of tumors, short (sTL), medium (mTL) and long telomere length (ITL), with 18 patients in each group. Telomere length was compared by ANOVA. Intra-group comparison achieved significant differences in telomere length among tumors from these three groups ($P < .001$), but not among adjacent or distant tissues (Figure 1A, lower panel).

Based on this classification, association between telomere length and clinicopathological characteristics was analyzed. Correlation was found between tumor histology and telomere length ($P = .049$) (Table 1). Most moderately and poorly differentiated tumors showed short telomeres, but well-differentiated tumors mostly contained long telomeres. We further utilized the average telomere length of all 'normal' tissues as a reference, and defined short or long telomere groups based on whether the T/S ratio of the tumors was lower or higher than the average T/S ratio of 'normal' tissues respectively. We found an inverse correlation between telomere length and tumor size ($P = .047$, Table S2), confirming our observation that tumors with short telomeres were relatively larger.

To see whether tumors with short telomeres are enriched for CSLC signatures, we systematically compared the expression of CD44, EPHB2 and LGR5 by immunostaining in tumors with short and long telomeres. CD44 is a prominent WNT signaling target in the intestine and is selectively expressed on the renewing epithelial cells lining the crypts [49]. The expression of CD44 is elevated in cancer stem-like cells in cancer including colon and gastric cancer [50]. Expectedly, CD44 was expressed at the bottom of normal crypt at very low levels (an average of 2.4-8%), but was much higher in tumors than in distant normal tissues from both the sTL and ITL groups (Figure 2A). The average percentage of CD44 positive cells was 21% in sTL tumors, significantly higher than that of ITL tumors with less than 10% (Figure 2B). Another Wnt target gene, the

Figure 1. Telomere length of tumors, adjacent and distant tissues, and blood.(A) Scatter plot displaying telomere lengths shown as T/S ratio by qPCR. Fifty-four patients are ranked in ascending order by telomere lengths of tumor tissues. Bar = mean ± s.e.m., n = 4 technical replicates. Differences among short, medium and long groups shown underneath are represented as mean ± SD.(B) Box plot showing distributions of relative telomere length.(C) TRF determination by Southern blot analysis. HEF, human embryonic fibroblasts. Samples were labeled with patient's sequential number (1-8, short telomeres; 46-54, longer telomeres).(D) Pearson correlation shows a high correlation of TRF with T/S ratio.(E) Telomere fluorescence signal by QFISH in tumor with short telomeres and distant 'normal' tissues from the same patient. Nuclei were counterstained in blue by DAPI. Scale bar = 20 μm.(F) Column scatter plots showing telomere length as fluorescence intensity of tumor (T) and distant 'normal' tissue (N) from six patients each group. Imaging fields and cells were randomly and evenly selected under the DAPI filter to see just nucleus to avoid of any possible bias. Black lines indicate the average value. Data are represented as mean ± SD. **, $P < .01$; ***, $P < .001$.

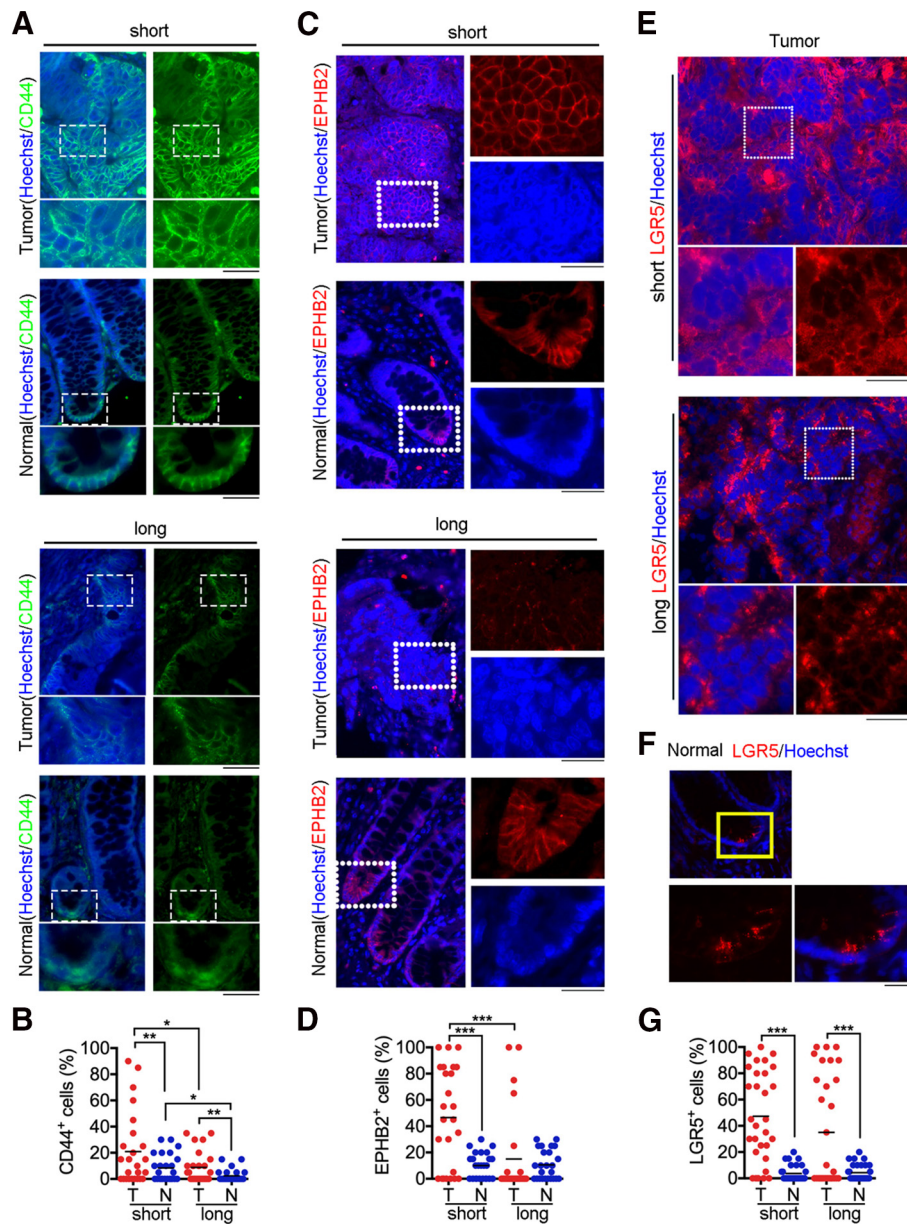


Figure 2. Short telomere tumors contain more cancer stem cell like cells (CSLCs).(A,C,E,F) Immunostaining of CD44, EPHB2, and LGR5 in the tumor and distant tissues of short and long telomere groups. Nuclei were counterstained by Hoechst 33342. Scale bar = 20 μ m.(B,D,G) Column scatter plot shows proportion of CD44, EPHB2, and LGR5 positive cells in the tumor and distant tissues of short and long telomere groups. *, $P < .05$; **, $P < .01$; ***, $P < .001$. T, tumor; N, distant 'normal' tissue.

receptor tyrosine kinase EphB2, is expressed in a decreasing gradient from the crypt base toward the differentiated cell compartment [51]. EPHB2 expression cells took about 10% of the normal crypt, but was heterogeneously expressed at higher levels in tumors of the sTL group (~46%) than in those of the lTL group (~15%) (Figure 2, C and D). LGR5 marks stem cells in normal intestine [52] and also is a functional marker in colorectal CSCs [9]. LGR5 expression is implicated in colorectal carcinogenesis, tumor cell growth and invasion [9,11,53]. Indeed, LGR5 was highly expressed in CRC tumors from both long and short telomere groups by immunofluorescence (IF) (Figure 2E), while LGR5 expression was consistently restricted to only a few cells in 'normal' crypt basal cells (Figure 2F). In addition, *in situ* staining of LGR5 (N-Terminal) shown as dot-like pattern in our study also is consistent with other studies [54,55].

LGR5 positive cells had a wide distribution in tumors of both telomere length groups (Figure 2G). The average percentage of LGR5 in sTL groups was slightly higher than that of lTL group, but significantly higher in long and short telomere tumors than that of normal tissues (around 4%). Although the reported percentage of tumor-initiating cells varies from 0.0001% to 25% [56,57], we observed higher frequency of CD44, EPHB2, LGR5 positive cells in the primary tumor sections, supported by previous studies [58,59].

These data show that CRC tumors with relatively short telomeres are enriched with more and heterogeneous CSLCs by various CSLC markers. Collectively, these results suggest that relatively short telomeres are associated with poorer differentiation, CSLCs and increased tumor volume/size, suggestive of their progressively higher proliferation.

Cell Proliferation and Telomere Length Connection in CRC Tumors

Cell proliferation tightly correlates with tumor growth and extension, as shown by expression of marker for proliferation Ki67 [60]. To validate the faster growth/higher proliferation state of sTL tumors, we carried out immunostaining of Ki67 and observed higher expression pattern in short telomere CRC tumors than ITL group tumors (Figure 3A). Ki67 positive cells were mainly located at the mid-crypt with frequency of about 10–15% of the whole crypt,

also well supported by literatures [55,61,62]. Nearly half of the sTL tumor cells were in highly proliferative state, whereas the ITL tumors showed low level of Ki67 similar to normal tissues, indicating a slower tumor progression rate. Also, we conducted analysis of cell proliferation using proliferating cell nuclear antigen (PCNA) [63]. Again, tumor cells had more proliferative cells than did normal cells, and the short telomere tumors contained more proliferative cells than did normal tissues and long telomere tumors (Figure 3B).

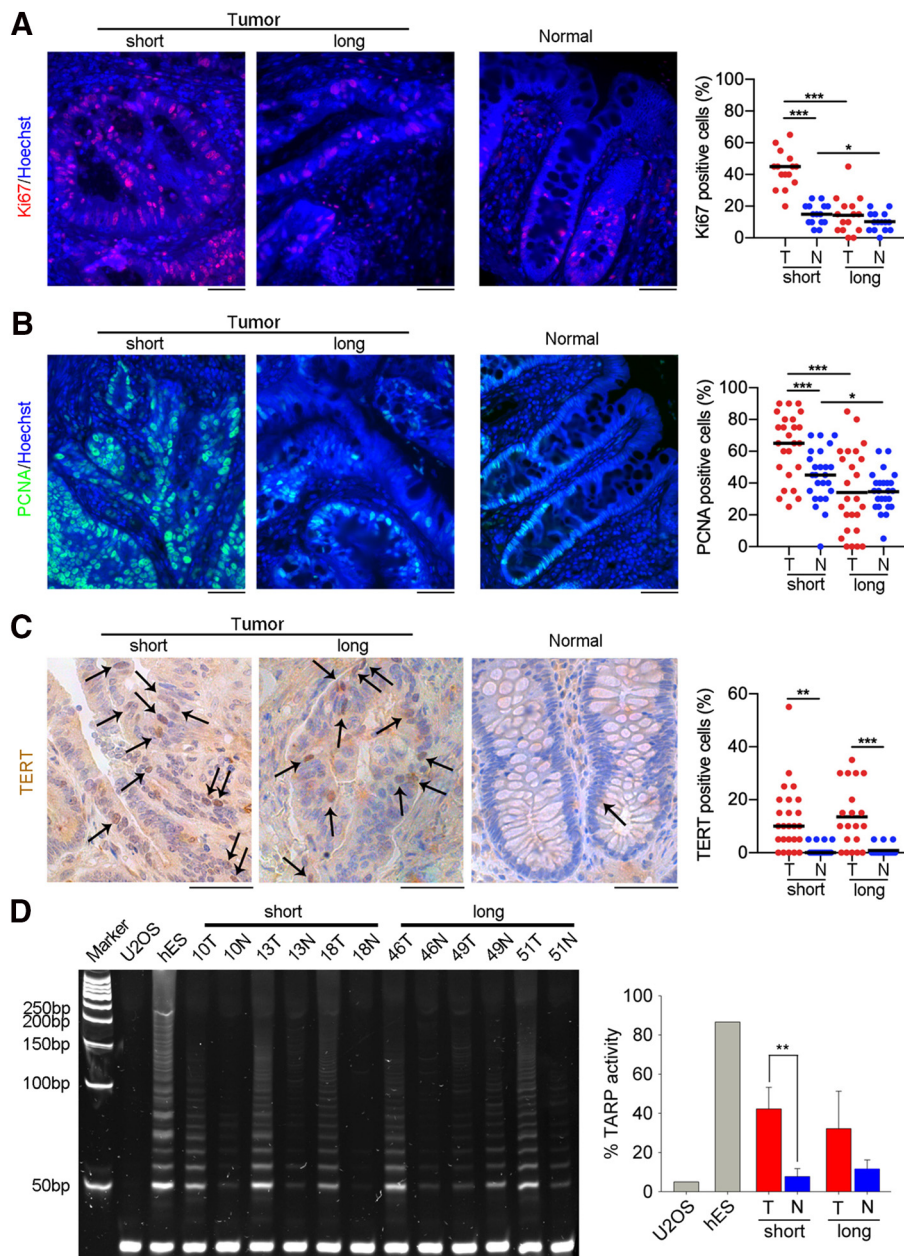


Figure 3. Short telomere tumors show higher proliferation.(A) Immunostaining and quantification of Ki67 in tumor and distant normal tissues. Scale bar = 50 μm.(B) Immunostaining and quantification of PCNA in tumor and distant normal tissues. Scale bar = 50 μm.(C) Immunohistochemistry staining and quantification of TERT in tumor and distant normal tissues. Scale bar = 50 μm. Arrows indicate TERT positive cells.(D) Telomeric Repeat Amplification Protocol (TRAP) Assay of telomerase activity in tumor and normal tissues from short and long telomere groups. Right panel, relative quantification of telomerase activity. The bottom bands indicate internal control used to calibrate PCR efficiency. U2OS and human embryonic stem (hES) cell line WA26 served telomerase negative and positive controls, respectively. *, $P < .05$; **, $P < .01$; ***, $P < .001$. T, tumor; N, distant 'normal' tissue.

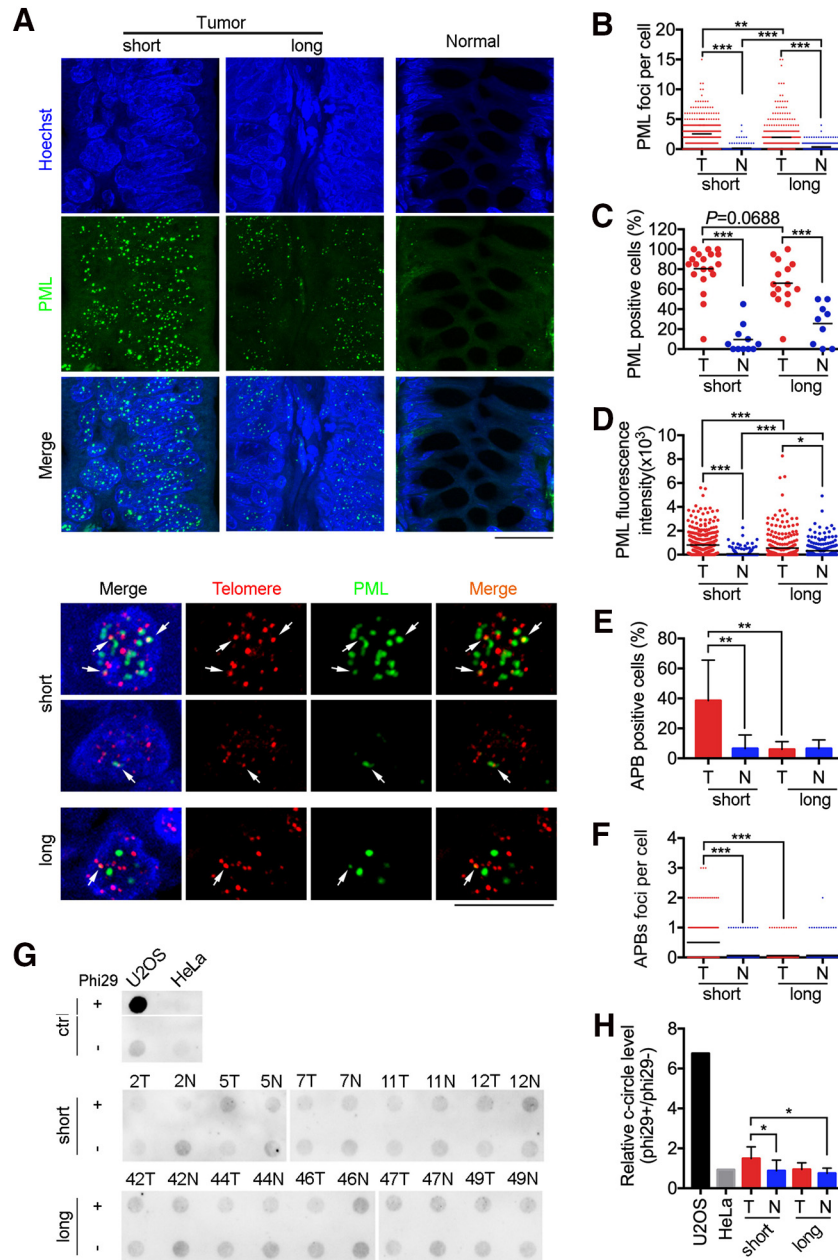


Figure 4. High incidence of PML and APBs in tumors with short telomeres.(A) Immunofluorescence of PML expression (Upper panel). Nuclei were counterstained with Hoechst 33342. Scale bar = 20 μ m. Lower panel, Immunofluorescence of APB foci in tumor from short and long telomere groups. Scale bar = 10 μ m.(B) Quantification of PML expression levels by counting PML foci per cell.(C) Proportion of PML foci positive cells.(D) PML expression levels estimated by fluorescence intensity.(E) Proportion of APB foci positive cells. Bar = mean \pm SD.(F) Number of APB foci per cell. The black line indicates the average value. Comparisons were made by mean \pm SD.(G) C-circle assay of primary tumor and distant normal tissues. U2OS and HeLa served as positive and negative controls, respectively. (H) Quantification of relative c-circle level of tissues from short (n = 5) and long (n = 5) telomere groups. Bar = mean \pm s.e.m. *, $P < .05$; **, $P < .01$; ***, $P < .001$. T, tumor; N, distant 'normal' tissue.

To understand the underlying mechanisms of telomere maintenance, we firstly analyzed expression of key telomerase genes *TERT* and *TERC*. hTERT was detected at high expression levels in tumors, and strongly and heterogeneously expressed in restricted subsets of tumor cells by immunohistochemistry (IHC), compared with epithelial cells in distant 'normal' tissues with *TERT* expression at relatively low levels (Figure 3C). The number of *TERT* positive cells was notably higher in tumors of both sTL and lTL groups than in corresponding distant normal tissues (Figure

3C), consistent with the well-established notion that tumors express high telomerase.

We analyzed the potential correlation between telomere length and *TERT* or *TERC* expression levels using more samples including randomly selected mTL group samples (Figure S2A–S2C). By qPCR, expression levels of *TERT* or *TERC* varied among tumors and normal tissues and did not differ between sTL and lTL groups (Figure S2B and S2C). Additionally, expression levels of *TERT* or *TERC* did not correlate with their telomere lengths regardless of tumors or normal

tissues (Figure S2D). Nevertheless, telomeric repeat amplification protocol (TRAP) assay demonstrated that telomerase activity of tumors was higher than that of normal tissues in both short and long groups (Figure 3D), consistent with more TERT positive cells in tumors by IHC (Figure 3C). As a control, U2OS did not express telomerase activity, whereas hES cells expressed high telomerase activity, and this was also supported by specific IHC assay of TERT (Figure S2E). These results suggest that telomerase is implicated in telomere maintenance of tumors but telomerase alone could not explain the telomere length variations in colorectal tumors.

PML Expression and Telomere Heterogeneity and Maintenance

PML plays a crucial role in cancer cell immortalization by promoting the alternative lengthening of telomeres (ALT) mechanism

[64]. To test whether PML is potentially involved in telomere length maintenance and heterogeneity in clinical CRC specimens, we analyzed expression of PML by immunofluorescence microscopy. PML protein was highly expressed in tumors and only weakly expressed in a small subset of cells in distant normal crypts (Figure 4A, upper panel). Tumors of the sTL group exhibited PML foci at much higher frequency (2.55 ± 2.19) than did cells (0.14 ± 0.51) in distant crypt (Figure 4B). Frequency of PML foci also was higher in tumors of the lTL group than that of the bottom crypt (1.98 ± 2.56 versus 0.37 ± 0.71), but lower than that of tumors from the sTL group ($P = .0015$). The large standard derivation implies that PML expression also is heterogeneous in CRC tumors.

Moreover, proportion of PML positive cells was remarkably higher in tumors of the sTL group than that of distant normal crypt (an average of 81% versus 10%), and differed between tumor and normal

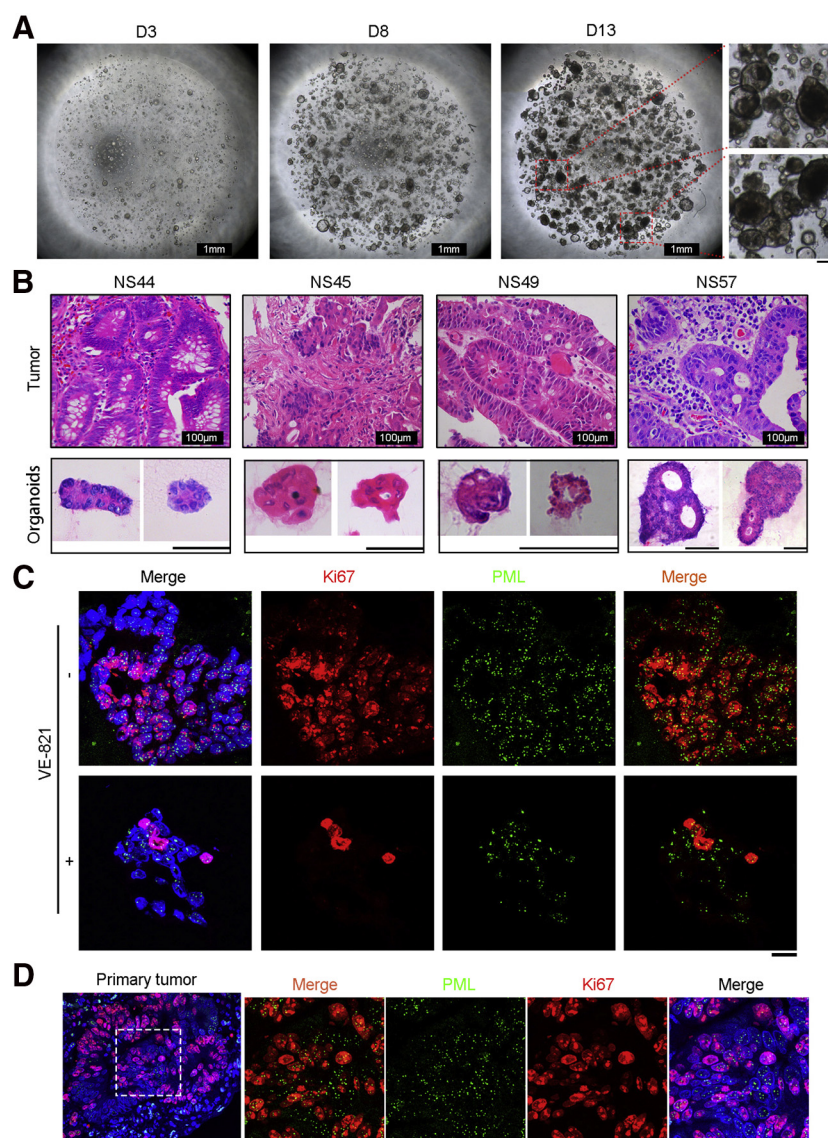


Figure 5. Characterization of organoids developed from CRC tumors and treatment by ATR inhibitor, VE-821. (A) Phase-contrast image showing growth of CRC organoid cultured from day 3 to day 13. Scale bar = $200 \mu\text{m}$. (B) Representative images of hematoxylin and eosin (H&E) staining of primary tumor and the tumor-derived organoids. NS44, NS49, and NS57 belong to short TL tumors, and the NS45 to middle-long TL tumors. Scale bar = $50 \mu\text{m}$. (C) Immunofluorescence microscopy of Ki67 and PML in organoids treated with VE-821 or DMSO served as dissolvent control. Scale bar = $20 \mu\text{m}$. (D) Immunofluorescence microscopy of Ki67 and PML in primary tumor. Scale bar = $20 \mu\text{m}$.

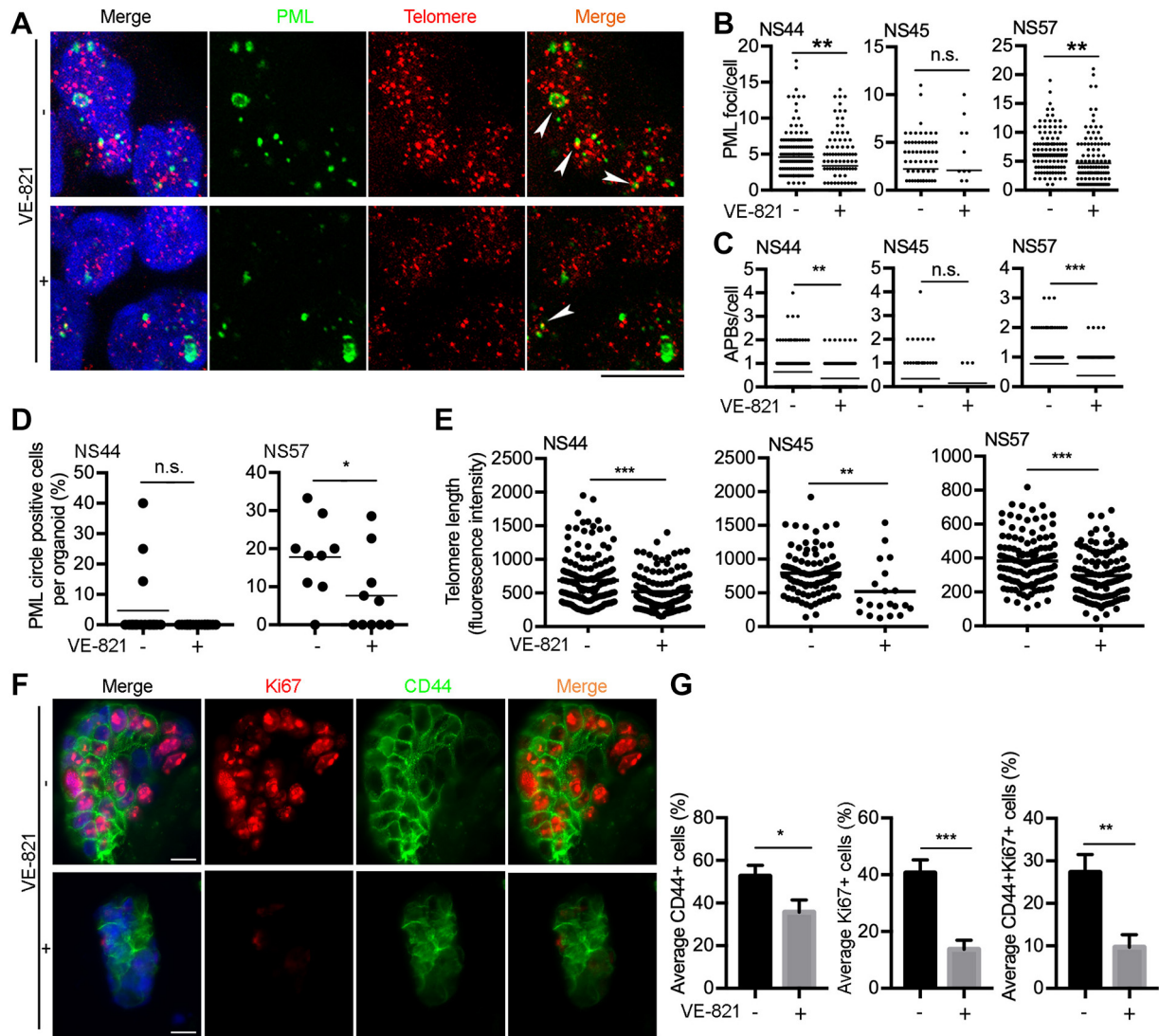


Figure 6. VE-821 reduces PML and telomere lengths and proliferative CSLCs of organoids.(A) Representative IF-FISH of PML and telomere in organoids treated with VE-821 compared with control. White arrows indicate APBs. Scale bar = 10 μ m.(B,C) Quantification of PML foci (B) and APBs (C) per cell in organoids treated with VE-821 compared with control.(D) Proportion of PML circle positive cells per organoid.(E) Relative telomere length shown as fluorescence intensity in cells of organoids.(F) Immunofluorescence microscopy of Ki67 and CD44 in organoids. Scale bar = 20 μ m.(G) Frequency (%) of CD44⁺, Ki67⁺, or CD44⁺Ki67⁺ double-positive cells in organoids treated with or without VE-821. Bar = mean \pm s.e.m.; n > 30 organoids analyzed from 4 patients. *, $P < .05$; **, $P < .01$; ***, $P < .001$.

crypt in the ITL group (Figure 4C). Moreover, PML foci exhibited stronger fluorescence intensity, suggestive of high expression levels, in tumors of the sTL than did the ITL group, or the normal crypts (Figure 4D).

Notably, cells expressing high levels of PML also exhibited high proliferation as indicated by strong nuclear expression of Ki67. More cells with high expression of both PML and Ki67 were found in the sTL group than in the ITL group or in distant tissues (Figure S3A and S3B). Yet, CSLCs marked by LGR5 or EPHB2 expressed PML at levels similar to those of LGR5⁻ or EPHB2⁻ cells in the tumor (Figure S3C-S3F).

Assembly of ALT-associated PML nuclear bodies (APBs) at telomeres is a hallmark of human ALT-positive cells [29,31]. Analysis by standard IF-FISH of APBs showed that more APB positive cells and a higher incidence of APB foci were observed in tumors with

short telomeres than in distant tissues or in tumors with longer telomeres ($P < .001$) (Figure 4A lower panel, 4E and F). PML expression may play a role in telomere maintenance of proliferative cancer cells.

C-circle assays measure C-circles as responsive and specific markers of ALT activity [65]. We carried out the C-circle assay using tumor and normal tissues (Figure 4G). Given that the tissue mass is actually a population of heterogeneous cells which would contain both C-circle positive cells and negative cells, it is expected to see higher C-circle level of pure ALT positive U2OS cell line than other cell types. We observed more and heterogeneous C-circles in sTL tumors, with frequency relatively higher than that of both normal tissues and C-circle negative HeLa cell line, suggesting possible ALT pathway in some cells of sTL tumors (Figure 4H).

Targeting PML/APBs Diminishes Proliferation of CSLCs and Development of Patient-Derived Organoids

PML is essential for APBs assembly and further provides a platform for DNA damage response and repair factors and homologous recombination proteins, including replication protein A (RPA), RAD51, RAD52 [66]. The number of PML associated with DNA damage is under the control of NBS1, ATM, Chk2 and ATR [67]. Patient-derived organoids (PDOs) have recently emerged as robust models to mimic *in vivo* experiments and predict clinical outcomes in patients [41–44]. To disrupt PML/APBs in organoids, we used an ATR inhibitor VE-821, as protein kinase ATR is a critical regulator of recombination recruited by RPA. ATR inhibitor has been proved to be hypersensitive to ALT pathway mediated by recombination [68,69]. To mimic the *in vivo* response of VE-821 treatment, we cultured organoids according to the well-established protocols [41,47] (Figure 5A). Histological evaluation initially revealed morphological similarities between organoids and the primary tumor biopsies from which they were originally derived (Figure 5B). The half-maximal inhibitory concentration (IC50) of VE-821 for the NS57 organoids in our experiments was 3.2 μM , and we used this concentration for all subsequent experiments (Figure S4A and S4B). Previous comparison of a panel of cell lines showed substantially higher levels of IC50 in the telomerase-positive cell lines than in the ALT cell lines [68], suggesting that VE-821 would also inhibit those telomerase positive cells but with an obviously higher IC50 concentration ($\sim 9 \mu\text{M}$). The concentration (3.2 μM) used here is far below from that of telomerase positive cell lines. We compared responses to VE-821 in organoids from four patients. Initially, we measured the number and size of organoids upon treatment (Figure S4C and S4D). Organoid size was notably reduced following treatment with VE-821 of all samples (Figure S4D). To confirm the effect of VE-821 on inhibition of PML, we carried out western blot assay and showed reduced PML levels in HCT116 cell lines following treatment of VE-821 with increasing concentrations (Figure S4E).

VE-821 reduced cell proliferation and PML foci in organoids (Figure 5C). Additional staining of PML and Ki67 in primary biopsy confirmed that expression pattern of PML and Ki67 in the parental tumors was maintained in organoids (Figure 5D). Further immunostaining of PML followed by telomere FISH showed a significant decrease in PML foci by VE-821, and also reduced PML circles, which represent the classical larger PML nuclear body structure, or APBs (Figure 6, A–D). Meanwhile, VE-821 treatment also expectedly shortened telomeres in these organoids (Figure 6E), and yet did not obviously change TERT expression (Figure S4F).

To assess whether PML and CSLCs are implicated in organoid development, we performed immunostaining of CD44&Ki67 and assessed proportion of CSLCs and proliferative cells. Proportion of CSLCs and especially proliferative CSLCs was notably reduced in organoids by VE-821 (Figure 6, F and G).

Discussion

Here we validate that most CRC tumors exhibit short telomeres compared with normal tissues from the same patient. Moreover, tumors with shorter telomeres exhibit poor differentiation and are associated with larger CRC tumors and a high proliferation state. An *In silico* computational model of tumor growth and evolution demonstrates that cell proliferation potential is the strongest modulator of tumor growth [70]. The fast-growing evolving tumor was more than 6 times larger with 170 times more CSLCs than the

largest non-evolving control tumor [70]. Consistently, short telomere CRC tumors with large size contain more CSLCs marked by CD44, EPHB2, or LGR5. In agreement, cancers with “ever-shorter telomeres” proved to be highly aggressive [71], but longer telomeres are significantly associated with reduced colon cancer risk [72].

Human cells progressively lose telomeres with each cell division and also with age. Short telomeres initially can lead to cell senescence. Reactivation of telomerase permits cells to continue to proliferate and to achieve immortalization, and is a critical step in cancer progression [73]. We find similar levels of telomerase in sTL and ITL tumors, which is not matched with the faster cell turn-over rate of sTL tumors than ITL tumors. ALT can be activated after telomerase inhibition and also in human telomerase-positive cancer cells [74–76]. We find high expression of PML in CRC tumors with short telomeres. Presumably, PML/APBs revealed in the CRC tumors could be part of ALT pathway for telomere maintenance to prevent telomere from shortening further, and to achieve malignant growth. Extremely long or short telomeres as observed in typical ALT-positive U2OS cells are not obvious in the tumors of CRC, and this could be partly due to the heterogeneity of tumor cells and/or the co-existence of telomerase that could inhibit the classical ALT phenotype [77–81].

PML, not only mediates alternative lengthening of telomeres, but also engages in multiple cellular activities including DNA damage sensing and DNA repair [82]. One possible explanation for the high expression of PML in sTL tumor is that, in case of insufficient telomere maintenance of those short telomere tumors, cells would eventually enter “crisis”. In such cases, telomeres are so short that end-end chromosome fusions occur, followed by chromosome breakage-fusion-bridge events that lead to genomic instability [83]. Telomere DNA damage could increase the number of PML and eventually provide a favorable platform for ALT. PML itself can contribute to maintenance of telomeric chromatin integrity [84], and promotes their alternative lengthening [64]. In addition, the phenomenon that more PML/APBs in shorter telomere tumors in our study could be partly explained by early literatures which revealed short telomeres display an increased mobility in the nucleus and explore a larger nuclear volume, which could facilitate collisions with PML, thus the formation of APBs benefit from the accumulation of soluble PML protein at a telomere [85,86].

We show that expression of telomerase and PML together are implicated in telomere maintenance of colorectal tumor. Inhibition of the ALT pathway by decreasing PML/APBs further shortens telomeres and reduces proliferation of CSLCs and development of patient-derived organoids. The model of CRC tumor progression and telomere heterogeneity could narrow down therapeutic targets to improve cancer prevention and treatment. Further understanding of the molecular basis underlying PML-associated telomere maintenance together with telomerase inhibition may prove more effective in eradicating CRC tumors.

Supplementary data to this article can be found online at <https://doi.org/10.1016/j.tranon.2019.05.010>.

Authors' Contributions

P.G. conducted T/S ratio, clinicopathological data analysis and most FISH, IF and IHC experiments, functional experiments, analyzed data, interpreted results, and drafted the manuscript; H.W. conducted TRF, functional experiments and analyzed data, interpreted results, and drafted the manuscript; J.S.Z. assisted

experiments, analyzed data and interpreted results; Y.D.F. conducted most experiments, analyzed data, interpreted results, and drafted the manuscript; Z.M.Z. advised and helped statistical analysis; J.M.W., Y.Y., H.Y.W., Z.C.Z., J.Y., L.L.L., M.G., M.Z. and J.H.Y. performed some experiments and provided technical support; F.W., R.X., X.H.P. and S.W. discussed and interpreted results and revised the manuscript; L.L. and F.Q. designed the experiments, interpreted results and wrote and revised the manuscript.

Acknowledgements

We thank Qiang Zhao, Feixiang Ge and Zhongzhi Zhao for assisting experiments, and Jian Yu for critical reading and revision of the manuscript, and Xiamen Multi Dimension Biomedical Technology Co.,Ltd. for help with telomerase activity assay. This study was supported by funding from China Ministry of Science and Technology Program of International S&T Cooperation (2014DFA30450).

Conflict of interest

None.

References

- Torre LA, Bray F, Siegel RL, Ferlay J, Lortet-Tieulent J, and Jemal A (2015). Global cancer statistics, 2012. *CA Cancer J Clin* **65**, 87–108.
- Kreso A and Dick JE (2014). Evolution of the cancer stem cell model. *Cell Stem Cell* **14**, 275–291.
- Meacham CE and Morrison SJ (2013). Tumour heterogeneity and cancer cell plasticity. *Nature* **501**, 328–337.
- Pattabiraman DR and Weinberg RA (2014). Tackling the cancer stem cells — what challenges do they pose? *Nat Rev Drug Discov* **13**, 497–512.
- Tang DG (2012). Understanding cancer stem cell heterogeneity and plasticity. *Cell Res* **22**, 457–472.
- Kreso A, van Galen P, Pedley NM, Lima-Fernandes E, Frelin C, Davis T, Cao L, Baizitov R, Du W, and Sydorenko N, et al (2014). Self-renewal as a therapeutic target in human colorectal cancer. *Nat Med* **20**, 29–36.
- Medema JP (2013). Cancer stem cells: the challenges ahead. *Nat Cell Biol* **15**, 338–344.
- Zeuner A, Todaro M, Stassi G, and De Maria R (2014). Colorectal cancer stem cells: from the crypt to the clinic. *Cell Stem Cell* **15**, 692–705.
- Barker N, Ridgway RA, van Es JH, van de Wetering M, Begthel H, van den Born M, Danenberg E, Clarke AR, Sansom OJ, and Clevers H (2009). Crypt stem cells as the cells-of-origin of intestinal cancer. *Nature* **457**, 608–611.
- Du L, Wang H, He L, Zhang J, Ni B, Wang X, Jin H, Cahuzac N, Mehrpour M, and Lu Y, et al (2008). CD44 is of functional importance for colorectal cancer stem cells. *Clin Cancer Res* **14**, 6751–6760.
- Merlos-Suarez A, Barriga FM, Jung P, Iglesias M, Cespedes MV, Rossell D, Sevillano M, Hernando-Mombolona X, da Silva-Diz V, and Munoz P, et al (2011). The intestinal stem cell signature identifies colorectal cancer stem cells and predicts disease relapse. *Cell Stem Cell* **8**, 511–524.
- O'Brien CA, Pollett A, Gallinger S, and Dick JE (2007). A human colon cancer cell capable of initiating tumour growth in immunodeficient mice. *Nature* **445**, 106–110.
- Ricci-Vitiani L, Lombardi DG, Pilozzi E, Biffoni M, Todaro M, Peschle C, and De Maria R (2007). Identification and expansion of human colon-cancer-initiating cells. *Nature* **445**, 111–115.
- Hankey W, McIlhatton MA, Ebode K, Kennedy B, Hancioglu B, Zhang J, Brock GN, Huang K, and Groden J (2018). Mutational mechanisms that activate Wnt signaling and predict outcomes in colorectal cancer patients. *Cancer Res* **78**, 617–630.
- Saigusa S, Inoue Y, Tanaka K, Toiyama Y, Kawamura M, Okugawa Y, Okigami M, Hiro J, Uchida K, and Mohri Y, et al (2013). Significant correlation between LKB1 and LGR5 gene expression and the association with poor recurrence-free survival in rectal cancer after preoperative chemoradiotherapy. *J Cancer Res Clin Oncol* **139**, 131–138.
- Saigusa S, Inoue Y, Tanaka K, Toiyama Y, Matsushita K, Kawamura M, Okugawa Y, Hiro J, Uchida K, and Mohri Y, et al (2012). Clinical significance of LGR5 and CD44 expression in locally advanced rectal cancer after preoperative chemoradiotherapy. *Int J Oncol* **41**, 1643–1652.
- Hackett JA, Feldser DM, and Greider CW (2001). Telomere dysfunction increases mutation rate and genomic instability. *Cell* **106**, 275–286.
- O'Sullivan JN, Bronner MP, Brentnall TA, Finley JC, Shen WT, Emerson S, Emond MJ, Gollahon KA, Moskovitz AH, and Crispin DA, et al (2002). Chromosomal instability in ulcerative colitis is related to telomere shortening. *Nat Genet* **32**, 280–284.
- Roger L, Jones RE, Heppel NH, Williams GT, Sampson JR, and Baird DM (2013). Extensive telomere erosion in the initiation of colorectal adenomas and its association with chromosomal instability. *J Natl Cancer Inst* **105**, 1202–1211.
- Artandi SE, Chang S, Lee SL, Alson S, Gottlieb GJ, Chin L, and DePinho RA (2000). Telomere dysfunction promotes non-reciprocal translocations and epithelial cancers in mice. *Nature* **406**, 641–645.
- Rudolph KL, Millard M, Bosenberg MW, and DePinho RA (2001). Telomere dysfunction and evolution of intestinal carcinoma in mice and humans. *Nat Genet* **28**, 155–159.
- Baichoo E and Boardman LA (2014). Toward a molecular classification of colorectal cancer: the role of telomere length. *Front Oncol* **4**, 158.
- Greaves M and Maley CC (2012). Clonal evolution in cancer. *Nature* **481**, 306–313.
- Palm W and de Lange T (2008). How shelterin protects mammalian telomeres. *Annu Rev Genet* **42**, 301–334.
- Wright WE, Piatyszek MA, Rainey WE, Byrd W, and Shay JW (1996). Telomerase activity in human germline and embryonic tissues and cells. *Dev Genet* **18**, 173–179.
- Hahn WC and Weinberg RA (2002). Rules for making human tumor cells. *N Engl J Med* **347**, 1593–1603.
- Kim NW, Piatyszek MA, Prowse KR, Harley CB, West MD, Ho PL, Coviello GM, Wright WE, Weinrich SL, and Shay JW (1994). Specific association of human telomerase activity with immortal cells and cancer. *Science* **266**, 2011–2015.
- Cesare AJ and Reddel RR (2010). Alternative lengthening of telomeres: models, mechanisms and implications. *Nat Rev Genet* **11**, 319–330.
- Draskovic I, Arnoult N, Steiner V, Bacchetti S, Lomonte P, and Londono-Vallejo A (2009). Probing PML body function in ALT cells reveals spatiotemporal requirements for telomere recombination. *Proc Natl Acad Sci U S A* **106**, 15726–15731.
- Heaphy CM, de Wilde RF, Jiao Y, Klein AP, Edil BH, Shi C, Bettgowda C, Rodriguez FJ, Eberhart CG, and Hebbar S, et al (2011). Altered telomeres in tumors with ATRX and DAXX mutations. *Science* **333**, 425.
- Yeager TR, Neumann AA, Englezou A, Huschtscha LI, Noble JR, and Reddel RR (1999). Telomerase-negative immortalized human cells contain a novel type of promyelocytic leukemia (PML) body. *Cancer Res* **59**, 4175–4179.
- Bertorelle R, Rampazzo E, Pucciarelli S, Nitti D, and De Rossi A (2014). Telomeres, telomerase and colorectal cancer. *World J Gastroenterol* **20**, 1940–1950.
- Engelhardt M, Albanell J, Drullinsky P, Han W, Guillem J, Scher HI, Reuter V, and Moore MA (1997). Relative contribution of normal and neoplastic cells determines telomerase activity and telomere length in primary cancers of the prostate, colon, and sarcoma. *Clin Cancer Res* **3**, 1849–1857.
- Garcia-Aranda C, de Juan C, Diaz-Lopez A, Sanchez-Pernaute A, Torres AJ, Diaz-Rubio E, Balibrea JL, Benito M, and Iniesta P (2006). Correlations of telomere length, telomerase activity, and telomeric-repeat binding factor 1 expression in colorectal carcinoma. *Cancer* **106**, 541–551.
- Gertler R, Rosenberg R, Stricker D, Friederichs J, Hoos A, Werner M, Ulm K, Holzmann B, Nekarda H, and Siewert JR (2004). Telomere length and human telomerase reverse transcriptase expression as markers for progression and prognosis of colorectal carcinoma. *J Clin Oncol* **22**, 1807–1814.
- Hastie ND, Dempster M, Dunlop MG, Thompson AM, Green DK, and Allshire RC (1990). Telomere reduction in human colorectal carcinoma and with ageing. *Nature* **346**, 866–868.
- Rampazzo E, Bertorelle R, Serra L, Terrin L, Candiotto C, Pucciarelli S, Del Bianco P, Nitti D, and De Rossi A (2010). Relationship between telomere shortening, genetic instability, and site of tumour origin in colorectal cancers. *Br J Cancer* **102**, 1300–1305.

- [38] Valls C, Pinol C, Rene JM, Buenestado J, and Vinas J (2011). Telomere length is a prognostic factor for overall survival in colorectal cancer. *Colorectal Dis* **13**, 1265–1272.
- [39] Boardman LA, Johnson RA, Viker KB, Hafner KA, Jenkins RB, Riegert-Johnson DL, Smyrk TC, Litzelman K, Seo S, and Gangnon RE, et al (2013). Correlation of chromosomal instability, telomere length and telomere maintenance in microsatellite stable rectal cancer: a molecular subclass of rectal cancer. *PLoS One* **8**:e80015.
- [40] Heaphy CM, Subhawong AP, Hong SM, Goggins MG, Montgomery EA, Gabrielson E, Netto GJ, Epstein JI, Lotan TL, and Westra WH, et al (2011). Prevalence of the alternative lengthening of telomeres telomere maintenance mechanism in human cancer subtypes. *Am J Pathol* **179**, 1608–1615.
- [41] van de Wetering M, Francies HE, Francis JM, Bounova G, Iorio F, Pronk A, van Houdt W, van Gorp J, Taylor-Weiner A, and Kester L, et al (2015). Prospective derivation of a living organoid biobank of colorectal cancer patients. *Cell* **161**, 933–945.
- [42] Vlachogiannis G, Hedayat S, Vatsiou A, Jamin Y, Fernandez-Mateos J, Khan K, Lampis A, Eason K, Huntingford I, and Burke R, et al (2018). Patient-derived organoids model treatment response of metastatic gastrointestinal cancers. *Science* **359**, 920–926.
- [43] Fujii M, Shimokawa M, Date S, Takano A, Matano M, Nanki K, Ohta Y, Toshimitsu K, Nakazato Y, and Kawasaki K, et al (2016). A colorectal tumor organoid library demonstrates progressive loss of niche factor requirements during tumorigenesis. *Cell Stem Cell* **18**, 827–838.
- [44] Yan HHN, Siu HC, Law S, Ho SL, Yue SSK, Tsui WY, Chan D, Chan AS, Ma S, and Lam KO, et al (2018). A comprehensive human gastric cancer organoid biobank captures tumor subtype heterogeneity and enables therapeutic screening. *Cell Stem Cell* **23**, 882–897 e811.
- [45] Cawthon RM (2002). Telomere measurement by quantitative PCR. *Nucleic Acids Res* **30**, e47.
- [46] Herrera E, Samper E, and Blasco MA (1999). Telomere shortening in mTR^{-/-} embryos is associated with failure to close the neural tube. *EMBO J* **18**, 1172–1181.
- [47] Sato T, Stange DE, Ferrante M, Vries RG, Van Es JH, Van den Brink S, Van Houdt WJ, Pronk A, Van Gorp J, and Siersema PD, et al (2011). Long-term expansion of epithelial organoids from human colon, adenoma, adenocarcinoma, and Barrett's epithelium. *Gastroenterology* **141**, 1762–1772.
- [48] Tahara T, Shibata T, Okubo M, Kawamura T, Sumi K, Ishizuka T, Nakamura M, Nagasaka M, Nakagawa Y, and Ohmiya N, et al (2015). Telomere length in non-neoplastic colonic mucosa in ulcerative colitis (UC) and its relationship to the severe clinical phenotypes. *Clin Exp Med* **15**, 327–332.
- [49] Zeilstra J, Joosten SP, Dokter M, Verwiel E, Spaargaren M, and Pals ST (2008). Deletion of the WNT target and cancer stem cell marker CD44 in Apc(Min/+) mice attenuates intestinal tumorigenesis. *Cancer Res* **68**, 3655–3661.
- [50] Zoller M (2011). CD44: can a cancer-initiating cell profit from an abundantly expressed molecule? *Nat Rev Cancer* **11**, 254–267.
- [51] Batle E, Henderson JT, Beghtel H, van den Born MM, Sancho E, Huls G, Meeldijk J, Robertson J, van de Wetering M, and Pawson T, et al (2002). Beta-catenin and TCF mediate cell positioning in the intestinal epithelium by controlling the expression of EphB/ephrinB. *Cell* **111**, 251–263.
- [52] Barker N, van Es JH, Kuipers J, Kujala P, van den Born M, Cozijnsen M, Haegbarth A, Korving J, Begthel H, and Peters PJ, et al (2007). Identification of stem cells in small intestine and colon by marker gene Lgr5. *Nature* **449**, 1003–1007.
- [53] Uchida H, Yamazaki K, Fukuma M, Yamada T, Hayashida T, Hasegawa H, Kitajima M, Kitagawa Y, and Sakamoto M (2010). Overexpression of leucine-rich repeat-containing G protein-coupled receptor 5 in colorectal cancer. *Cancer Sci* **101**, 1731–1737.
- [54] Sanchez-Danes A, Larsimont JC, Liagre M, Munoz-Couselo E, Lapouge G, Brisebarre A, Dubois C, Suppa M, Sukumaran V, and Del Marmol V, et al (2018). A slow-cycling LGR5 tumour population mediates basal cell carcinoma relapse after therapy. *Nature* **562**, 434–438.
- [55] Sugimoto S, Ohta Y, Fujii M, Matano M, Shimokawa M, Nanki K, Date S, Nishikori S, Nakazato Y, and Nakamura T, et al (2018). Reconstruction of the Human Colon Epithelium In Vivo. *Cell Stem Cell* **22**, 171–176 e175.
- [56] Quintana E, Shackleton M, Sabel MS, Fullen DR, Johnson TM, and Morrison SJ (2008). Efficient tumour formation by single human melanoma cells. *Nature* **456**, 593–598.
- [57] Vincent A and Van Seuning I (2012). On the epigenetic origin of cancer stem cells. *Biochim Biophys Acta* **1826**, 83–88.
- [58] Baker AM, Graham TA, Elia G, Wright NA, and Rodriguez-Justo M (2015). Characterization of LGR5 stem cells in colorectal adenomas and carcinomas. *Sci Rep* **5**, 8654.
- [59] Humphries A, Cereser B, Gay LJ, Miller DS, Das B, Gutteridge A, Elia G, Nye E, Jeffery R, and Poulsom R, et al (2013). Lineage tracing reveals multipotent stem cells maintain human adenomas and the pattern of clonal expansion in tumor evolution. *Proc Natl Acad Sci U S A* **110**, E2490–2499.
- [60] Gerdes J, Schwab U, Lemke H, and Stein H (1983). Production of a mouse monoclonal antibody reactive with a human nuclear antigen associated with cell proliferation. *Int J Cancer* **31**, 13–20.
- [61] Lipkin M, Bell B, and Sherlock P (1963). Cell proliferation kinetics in the gastrointestinal tract of man. I. Cell renewal in colon and rectum. *J Clin Invest* **42**, 767–776.
- [62] Potten CS, Kellett M, Rew DA, and Roberts SA (1992). Proliferation in human gastrointestinal epithelium using bromodeoxyuridine in vivo: data for different sites, proximity to a tumour, and polyposis coli. *Gut* **33**, 524–529.
- [63] Teixeira CR, Tanaka S, Haruma K, Yoshihara M, Sumii K, and Kajiyama G (1994). Proliferating cell nuclear antigen expression at the invasive tumor margin predicts malignant potential of colorectal carcinomas. *Cancer* **73**, 575–579.
- [64] Osterwald S, Deeg KI, Chung I, Parisotto D, Worz S, Rohr K, Erfle H, and Rippe K (2015). PML induces compaction, TRF2 depletion and DNA damage signaling at telomeres and promotes their alternative lengthening. *J Cell Sci* **128**, 1887–1900.
- [65] Henson JD, Cao Y, Huschtscha LI, Chang AC, Au AY, Pickett HA, and Reddel RR (2009). DNA C-circles are specific and quantifiable markers of alternative-lengthening-of-telomeres activity. *Nat Biotechnol* **27**, 1181–1185.
- [66] Nabetani A and Ishikawa F (2011). Alternative lengthening of telomeres pathway: recombination-mediated telomere maintenance mechanism in human cells. *J Biochem* **149**, 5–14.
- [67] Dellaire G, Ching RW, Ahmed K, Jalali F, Tse KC, Bristow RG, and Bazett-Jones DP (2006). Promyelocytic leukemia nuclear bodies behave as DNA damage sensors whose response to DNA double-strand breaks is regulated by NBS1 and the kinases ATM, Chk2, and ATR. *J Cell Biol* **175**, 55–66.
- [68] Flynn RL, Cox KE, Jeitany M, Wakimoto H, Bryll AR, Ganem NJ, Bersani F, Pineda JR, Suva ML, and Benes CH, et al (2015). Alternative lengthening of telomeres renders cancer cells hypersensitive to ATR inhibitors. *Science* **347**, 273–277.
- [69] Reaper PM, Griffiths MR, Long JM, Charrier JD, McCormick S, Charlton PA, Golec JM, and Pollard JR (2011). Selective killing of ATM- or p53-deficient cancer cells through inhibition of ATR. *Nat Chem Biol* **7**, 428–430.
- [70] Poleszczuk J, Hahnfeldt P, and Enderling H (2015). Evolution and phenotypic selection of cancer stem cells. *PLoS Comput Biol* **11**:e1004025.
- [71] Dagg RA, Pickett HA, Neumann AA, Napier CE, Henson JD, Teber ET, Arthur JW, Reynolds CP, Murray J, and Haber M, et al (2017). Extensive proliferation of human cancer cells with ever-shorter telomeres. *Cell Rep* **19**, 2544–2556.
- [72] Pellatt AJ, Wolff RK, Lundgreen A, Cawthon R, and Slattery ML (2012). Genetic and lifestyle influence on telomere length and subsequent risk of colon cancer in a case control study. *Int J Mol Epidemiol Genet* **3**, 184–194.
- [73] Shay JW and Wright WE (2011). Role of telomeres and telomerase in cancer. *Semin Cancer Biol* **21**, 349–353.
- [74] Brault ME and Autexier C (2011). Telomeric recombination induced by dysfunctional telomeres. *Mol Biol Cell* **22**, 179–188.
- [75] Hu J, Hwang SS, Liesa M, Gan B, Sahin E, Jaskieloff M, Ding Z, Ying H, Boutin AT, and Zhang H, et al (2012). Antitelomerase therapy provokes ALT and mitochondrial adaptive mechanisms in cancer. *Cell* **148**, 651–663.
- [76] De Vitis M, Berardinelli F, and Sgura A (2018). Telomere length maintenance in cancer: at the crossroad between Telomerase and Alternative lengthening of Telomeres (ALT). *Int J Mol Sci* **19**.
- [77] Cerone MA, Londono-Vallejo JA, and Bacchetti S (2001). Telomere maintenance by telomerase and by recombination can coexist in human cells. *Hum Mol Genet* **10**, 1945–1952.
- [78] Hu Y, Shi G, Zhang L, Li F, Jiang Y, Jiang S, Ma W, Zhao Y, Songyang Z, and Huang J (2016). Switch telomerase to ALT mechanism by inducing telomeric DNA damages and dysfunction of ATRX and DAXX. *Sci Rep* **6**:32280.
- [79] Perrem K, Colgin LM, Neumann AA, Yeager TR, and Reddel RR (2001). Coexistence of alternative lengthening of telomeres and telomerase in hTERT-transfected GM847 cells. *Mol Cell Biol* **21**, 3862–3875.
- [80] Wen J, Cong YS, and Bacchetti S (1998). Reconstitution of wild-type or mutant telomerase activity in telomerase-negative immortal human cells. *Hum Mol Genet* **7**, 1137–1141.

- [81] Wilkie AO, Lamb J, Harris PC, Finney RD, and Higgs DR (1990). A truncated human chromosome 16 associated with alpha thalassaemia is stabilized by addition of telomeric repeat (TTAGGG)_n. *Nature* **346**, 868–871.
- [82] Bernardi R and Pandolfi PP (2007). Structure, dynamics and functions of promyelocytic leukaemia nuclear bodies. *Nat Rev Mol Cell Biol* **8**, 1006–1016.
- [83] Shay JW (2016). Role of Telomeres and Telomerase in Aging and Cancer. *Cancer Discov* **6**, 584–593.
- [84] Chang FT, McGhie JD, Chan FL, Tang MC, Anderson MA, Mann JR, Andy Choo KH, and Wong LH (2013). PML bodies provide an important platform for the maintenance of telomeric chromatin integrity in embryonic stem cells. *Nucleic Acids Res* **41**, 4447–4458.
- [85] Jegou T, Chung I, Heuvelman G, Wachsmuth M, Gorisch SM, Greulich-Bode KM, Boukamp P, Lichter P, and Rippe K (2009). Dynamics of telomeres and promyelocytic leukemia nuclear bodies in a telomerase-negative human cell line. *Mol Biol Cell* **20**, 2070–2082.
- [86] Molenaar C, Wiesmeijer K, Verwoerd NP, Khazen S, Eils R, Tanke HJ, and Dirks RW (2003). Visualizing telomere dynamics in living mammalian cells using PNA probes. *EMBO J* **22**, 6631–6641.